Surface Water as a Mediator and Reporter of Adhesion at Aqueous Interfaces

Tasha Jarisz, Sandra Roy, and Dennis K. Hore

August 2018

The final publication is available at ACS Publications via:
https://doi.org/10.1021/acs.accounts.8b00258

Surface Water as a Mediator and Reporter of Adhesion at Aqueous Interfaces

Tasha Jarisz, Sandra Roy, and Dennis K. Hore*

Department of Chemistry, University of Victoria, Victoria, British Columbia, V8W 3V6, Canada

E-mail: dkhore@uvic.ca

Conspectus

Understanding the adsorption of molecules onto surfaces is integral to a wide variety of fields with scientific, engineering, and industrial applications. The surface-adsorbed structure is governed by the nature of the molecule, surface characteristics, and solution environment. There are therefore three critical interactions that govern adhesion: solvent–analyte, substrate–analyte, and substrate–solvent. The last two interactions require a surface-specific probe restricted to a few nanometers or less. This is particularly true of efforts to probe polymer surface structure without being overwhelmed by bulk polymer signal, or interfacial water structure in the presence of bulk water. Second-order nonlinear optical techniques are ideal probes of such interactions, as their reporting depth is determined by the polar arrangement of molecules (a break in the macroscopic inversion symmetry) rather than the penetration of the optical fields. This Account begins with an introduction of surface water structure from the perspective of a nonlinear probe. Details about the unique view of the water orientation distribution are discussed, and contrasted with information obtained from conventional vibrational techniques. The salient features of water next to model hydrophobic and hydrophilic

surfaces are discussed, in preparation for a discussion of solute interactions that follows. We then present three examples using a combination of linear and nonlinear vibrational spectroscopy and molecular dynamics simulations to illustrate how water is both a mediator and a marker of adhesion. The first is a study of amphipathic peptide adhesion onto hydrophobic and hydrophilic surfaces, characterizing the adsorbed structure in relation to the water surrounding the molecule and trapped near the surface. Water is found to be especially important in mediating adhesion to hydrophilic surfaces, where it aids in solvating the peptide as well as facilitating interactions with the surface. In the second example, we look at adhesion of a multi-component polymer adhesive using surface-bulk heterospectral correlation analysis, in which surface vibrational spectroscopy is combined with bulk infrared absorption to determine interfacial structure development during the evaporation of water. When acrylic acid is added to the polymer, there is a change in orientation of the polymer before an increase in population. This is opposite to what is observed when no additive is present. In our third example, we show how interfacial water provides a unique window into the surface microenvironment during bacterial adhesion, highlighting the role of solution conditions at the surface in cell attachment and biofilm growth. Changes in the nonlinear vibrational response of interfacial water reflect changes occurring in the pH and ionic strength only at the surface, due to the presence of polymeric adhesives secreted by the bacteria. These studies underline the importance of surface water in governing the structure of adhered molecules, in mediating changes in the interfacial environment as a result of adhesion, and provide insight into a nanoscale region that is otherwise difficult to query. They also illustrate the importance of combining surface-sensitive and bulk spectroscopic probes with computer modeling to gain a better understanding of the interplay between water and adsorbate structure.

1 Introduction

The solid-aqueous interface is one of the most abundant chemical systems on earth, yet its structural details remain poorly understood. Aqueous interfaces, including water, ice, electrolyte, and biological solutions are relevant to a wide variety of fields in chemistry. They play a role in all aspects of our atmospheric and oceanic environments,[1,2] in many technological applications ranging from oil extraction to phase-transfer catalysis,[3] and in most fundamental biochemical processes including respiration, ion transport, and protein folding.[4] The complexity of such interfaces is why this topic has been so widely studied these past decades; yet a consensus on the details of interfacial interactions remains elusive.

The unique physical and chemical properties of aqueous interfaces arise from the strong hydrogen bonding network between water molecules, together with the asymmetry introduced by the surface. As a result, the structure of interfacial water is typically distinct from that of bulk water in terms of the distribution of hydrogen bonding species and their coordination.[5] Furthermore, interaction of interfacial water molecules with surface functional groups, for example hydrogen bonding with O–H terminated oxide surfaces, stabilizes the interfacial hydration structure. Many of the properties of water near a solid surface are therefore analogous to the hydration layers around osmolytes.[6] The adsorption of solvated ions, polymers, solute, and biological molecules at the surface add further complexity to these systems. In this work we aim to show the importance of water in mediating adhesion, and illustrate how the response from interfacial water can be used to determine the extent, conformation, and mechanism of molecular adhesion to solid surfaces.

2 Water structure at solid surfaces: insights from experiments and simulations

It has been established that the nature of the solution environment (temperature, pH, ionic strength) has consequences on the bulk solubility and three-dimensional structure of the solutes.[7] In the bulk, each water molecule makes on average 3.6 hydrogen bonds with other water molecules.[8] It is this dynamic network of hydrogen bonds that gives water its unique chemical and physical properties, and in turn affects the solute environment. When it comes to studying molecules at surfaces, it therefore makes sense to start with an investigation of the solvent environment at those surfaces.

Consider a glass of water, frozen in time, then slicing through the center with an atomically-sharp knife passing between water molecules. Folding the system open at the cut plane, the two new surfaces present water molecules that have lost 50% of the their hydrogen bonding partners. If we unfreeze time, one can imagine that the water molecules at the surface might rearrange in order to make the best of their situation, maximizing the number of hydrogen bonds they can make with waters behind them in the direction of the bulk water phase. Although we have invoked some fantasy, our description very closely resembles what is achieved in a molecular dynamics simulation. In a typical case, a cube of water molecules is created on a computer, the energy of the system is computed via classical or quantum mechanical approaches, and the trajectory of each water molecule is computed over a very small step size, typically 1–2 fs. The energy of the ensemble is then re-evaluated to generate the coordinates for the next time step. Continuing over millions of iterations, sped up with the help of clusters of computers, the goal is to provide a description of the equilibrium state of the system. In the case of our bulk water simulation, we expect to end up with a density near 1 g/cm^3 at 25 °C and reproduce the well-established thermodynamic properties of water. However, after we achieve this state, we can then abruptly cut the system in half as described above, and introduce a solid surface at one of the faces of our simulation box. When the sys-

tem is allowed to re-equilibrate under these conditions, we have the opportunity to observe the water surface structure that results, and relate this to the properties of the solid surface we introduced. Fig. 1a illustrates the density and (Fig. 1b) tilt order parameter (degree of orientation of the molecule's C_{2v} axis with respect to the surface normal) as a function of distance from a model hydrophobic and hydrophilic surface (full details in Ref. 9). For a hydrophobic surface, a monotonic increase in water density is observed in moving towards the bulk water phase, with an orientation distribution that becomes isotropic after about 1 nm or 2–3 molecular layers. For water adjacent to a hydrophilic (OH-terminated surface), the density oscillates about the bulk value, and the accompanying orientation profile is much more complex. It should be noted that the fine details of the results are dependent on the choice of interaction potential. In particular, the width of the hydrophobic water depletion region for simple models tends to be slightly larger than what would be obtained for more realistic surfaces. However, the distinguishing features of hydrophilic and hydrophobic surfaces remain apparent.

While such simulations are invaluable for their predictive capabilities and the level of structural detail provided, we seek experimental tools that can validate these results and provide additional data on which to base the simulations. The primary challenge is finding a probe that can operate at the solid–liquid environment directly, can exclude all bulk water contributions from the signal, and is structurally-sensitive. For example, monolayers of water can be deposited onto solid substrates, but the structure of such vacuum–water–solid interfaces bears little resemblance to how water behaves at the surface in the presence of bulk water. Optical probes offer the least perturbation when accessing the buried solid–liquid interface. Among them, a subset of nonlinear optical techniques is of interest, those based on even orders of the electric susceptibility, $\chi^{(2)}$, $\chi^{(4)}$, etc. In general, the polarization

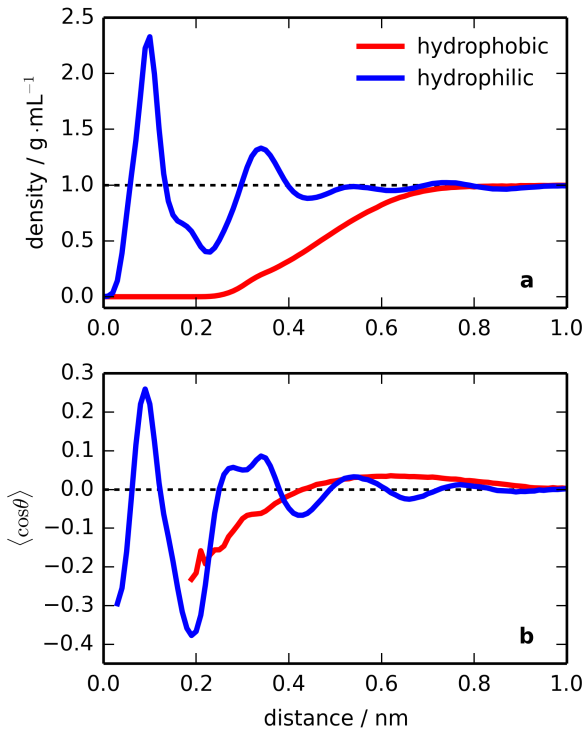

Figure 1: (a) Density and (b) average value of the tilt angle $\langle \cos\theta \rangle$ for water molecules adjacent to a hydrophobic (red) and hydrophilic (blue) surface. Adapted from Ref. 9. Copyright (2012) ACS Publications.

may be expressed as a series of contributions

$$\begin{aligned} P &= P^{(1)} + P^{(2)} + P^{(3)} + \cdots + P^{(n)} \\ &= \varepsilon_0 \left(\chi^{(1)} E + \frac{1}{2}\chi^{(2)} E^2 + \frac{1}{6}\chi^{(3)} E^3 + \cdots + \frac{1}{n!}\chi^{(n)} E^n \right) \end{aligned} \tag{1}$$

where ε_0 is the permittivity of free space, $\chi^{(n)}$ is the n^{th} order electric susceptibility, and E is the electric field at the surface, supplied by the probe lasers.[10] In order to understand why the even-ordered elements of $\chi^{(n)}$ are special in the context of surface water molecules, we consider the molecular origins of the susceptibility, the polarizability α, which can also be expanded in terms of linear and nonlinear contributions. The dipole moment can be expressed as

$$\begin{aligned} p &= p^{(1)} + p^{(2)} + p^{(3)} + \cdots + p^{(n)} \\ &= \alpha^{(1)} E + \alpha^{(2)} E^2 + \alpha^{(3)} E^3 + \cdots + \alpha^{(n)} E^n \end{aligned} \tag{2}$$

where the connection between the microscopic and macroscopic quantities can be realized as P is the sum over all molecules contributing their p. Returning to our analysis of the water tilt angle with respect to the surface normal, we now examine each of the terms in these sums. The first term is responsible for absorption; the imaginary part of $\alpha^{(1)}$ is the absorption coefficient. We can write

$$\begin{aligned} \chi^{(1)} &= \frac{1}{\varepsilon_0} \sum_{\text{molecules}} \alpha^{(1)} \\ &= N \langle \alpha^{(1)} \rangle \\ &= N \left(f_0 + f_2 \langle \cos^2 \theta \rangle \right) \alpha^{(1)} \end{aligned} \tag{3}$$

where N is the number of molecules and $\langle \alpha^{(1)} \rangle$ represents the average of $\alpha^{(1)}$ over all values of the tilt angle θ. If we consider the order parameters f_0 and f_1 we can see that the linear response is related to $\cos^2 \theta$, an important result for absorption spectroscopy. For simplicity,

consider that bulk water and surface water have the same properties at the molecular level, and that the two species differ only in terms of their orientation distribution. If we then have a probe beam that is absorbed by water, or if we perform a simulation and create a sum of $\cos^2\theta$ for each molecule, it will be very difficult to get a representative picture of the surface species since they will be drowned out by their bulk counterparts that appear in far greater numbers. The same situation is true for fluorescence or Raman scattering originating from the third-order response function[11]

$$\begin{aligned}\chi^{(3)} &= \frac{1}{\varepsilon_0}\sum_{\text{molecules}}\alpha^{(3)} \\ &= N\langle\alpha^{(3)}\rangle \\ &= N\left(f_0 + f_2\langle\cos^2\theta\rangle + f_4\langle\cos^4\theta\rangle\right)\alpha^{(3)}.\end{aligned} \tag{4}$$

We can generalize this discussion to conclude that all probes based on an odd-order response function probe only even powers of $\cos\theta$.

We now consider the lowest even-order response, the second order response, and find that

$$\begin{aligned}\chi^{(2)} &= \frac{1}{\varepsilon_0}\sum_{\text{molecules}}\alpha^{(2)} \\ &= N\langle\alpha^{(2)}\rangle \\ &= N\left(f_1\langle\cos\theta\rangle + f_3\langle\cos^3\theta\rangle\right)\alpha^{(2)}.\end{aligned} \tag{5}$$

From here the pattern is clear: techniques based on even orders of the susceptibility tensor are sensitive to odd powers of $\cos\theta$. Consider the electric field radiated from such a $P^{(2)}$ source. Fig. 2 illustrates that if the water molecule is flipped, we have $\theta \to 180^\circ - \theta$, and $\cos(180^\circ - \theta) = -\cos\theta$. This relation holds for any odd power of cosine. In other words, the field generated from two molecules with opposite orientations will destructively interfere in a $\chi^{(2)}$ process. As a result, there is no $P^{(2)}$ from any molecules in the bulk water phase on account of their isotropic distribution. At the surface, the orientation preference of water

molecules in response to their desire to maximize their hydrogen bonding opportunities will break this symmetry, and the light emitted from $P^{(2)}$ is detected.

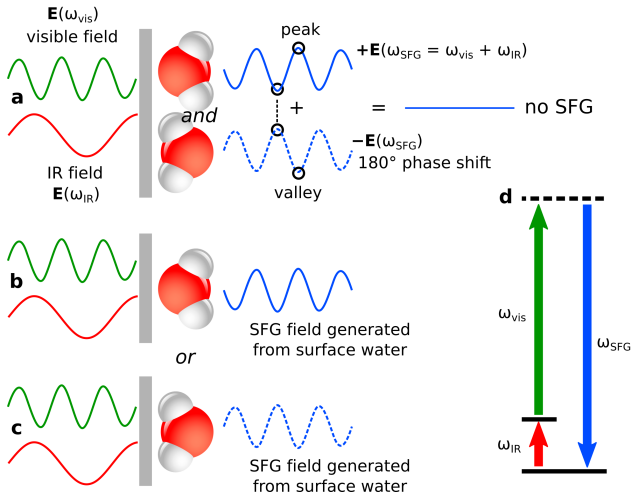

Figure 2: (a) In the bulk, light produced from the second order polarization destructively interferes with that from another molecule with opposite orientation, so no SFG can be measured from bulk water. At the surface, water has a preference for its orientation based on hydrogen bonding opportunities, so SFG is detected from these species, and the phase of the emitted field is shifted by 180° for molecules with their (b) oxygen or (c) hydrogen directed towards the surface. (d) An energy level diagram illustrating the process of sum-frequency generation.

Now that we have identified a surface-sensitive probe, we return to the structural question. We are most interested in techniques that can provide information on the interfacial water hydrogen bonding environment. For this reason, we use visible-infrared sum-frequency generation (SFG) where one of the probe lasers is at frequency ω_{vis} typically 18,797 cm^{-1} (532 nm), far from any electronic or vibrational resonance, and the other is tuned from $\omega_{\mathrm{IR}} = 2800$–$3800$ cm^{-1} to cover the distribution of O–H stretching frequencies. We detect the light emitted at the sum frequency $\omega_{\mathrm{vis}} + \omega_{\mathrm{IR}}$, and plot its intensity as a function of ω_{IR}. As shown in Fig. 2d, one advantage of this particular $\chi^{(2)}$ process is that the emitted light is at higher frequency than the visible laser beam, so there is no difficulty associated with fluorescence. Furthermore, for the range of frequencies listed above, the SFG appears between 442–463 nm, ideal for low-light level detectors with peak response in the blue/green. Another popular choice is to have ω_{vis} in the near-infrared near 800 nm, with SFG then pro-

duced in the 614–654 nm range. Fig. 3 illustrates example SFG spectra as collected from a hydrophobic (air) and hydrophilic (glass) surface, superimposed on the IR absorption spectra of bulk water and ice. One can see that the 3.6 hydrogen bonds per molecule in the bulk liquid takes the form of a wide distribution of hydrogen bonding environments, with a peak intensity near 3400 cm^{-1}. Ice has a tetrahedral structure, and correspondingly the absorption maximum is shifted to approximately 3200 cm^{-1}. SFG spectra of the hydrophobic and hydrophilic surfaces reveal the complexity of the interfacial hydrogen bonding environments, and the drastic differences between the two surfaces. This is a consequence of the substantial difference in density and orientation as revealed in the simulations. Water next to the hydrophilic surface exhibits significant intensity at 3200 and 3400 cm^{-1}, and the relative intensity of these O–H stretching bands is sensitive to the detailed surface characteristics.[12] At the hydrophobic surface, a sharp feature near 3700 cm^{-1} originates from uncoupled OH oscillators, water molecules with one OH bond directed towards a surface with no opportunity for hydrogen bonding.[13,14] Such fundamental studies of water next to model surfaces are important not only for understanding the neat water interfaces, but also in characterizing the perturbation of the structure upon the addition of solutes. In the following sections, we will provide some examples where molecular simulations together with SFG experiments provide insight into the role of water in dictating and revealing adhesion events.

3 Surface water as a mediator and reporter of adhesion at aqueous interfaces

3.1 Peptide adhesion

Synthetic peptides offer the possibility to study biomolecular interactions at a level of detail that is often not possible with proteins. Face-wise amphiphilic α-helices are particularly interesting due to their application as antimicrobial agents and role in membrane pore for-

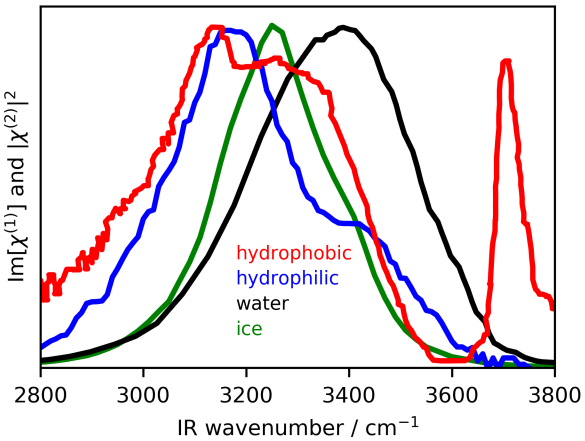

Figure 3: Im[$\chi^{(1)}$] for water (black)[15] and ice (green),[16] superimposed on $|\chi^{(2)}|^2$ for water at a hydrophobic (red)[5] and hydrophilic (blue)[17] surface. All spectra have been normalized to their highest intensity in this wavelength region in order to facilitate comparison of their shapes.

mation.[18] LKα14 is a 14-residue leucine- and lysine-containing peptide that forms a stable α-helix in solution.[19] Interactions between the adsorbed state of LKα14 and surfaces of varying hydrophobicity have been extensively studied by a variety of techniques, including SFG spectroscopy[20–23] and molecular simulations.[24,25] Early experiments have shown that when the peptide is adsorbed onto a hydrophilic surface, its lysine residue terminal NH_3^+ groups produce SFG signal, while the leucine terminal methyl stretching modes are silent.[21] On a hydrophobic surface, the opposite was observed, with only CH_3 groups producing SFG signal. It was proposed that on hydrophobic surfaces LKα14 adopts an orientation where its hydrophobic leucine residues are in contact with the surface and are therefore immobilized in a manner that breaks the centrosymmetry to provide the SFG response; on the hydrophilic surface the peptide is flipped. We followed up on this observation by performing some simulations of LKα14 with model hydrophobic and hydrophilic surfaces, including water and ions.[26] A snapshot from the two systems is shown in Fig. 4.

Using the peptide atomic coordinates from the MD trajectories, we constructed the predicted SFG response from the side chains. In agreement with the experimental observations, the hydrophobic adsorbed orientation and conformation produced only leucine signals, while

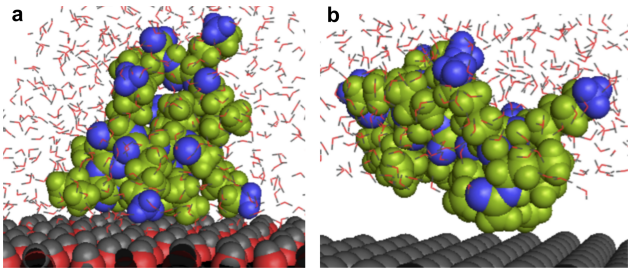

Figure 4: Snapshots of the peptide LKα14 adsorbed on a (a) hydrophilic and (b) hydrophobic surface. Adapted from Ref. 27. Copyright (2017) Elsevier.

the hydrophilic surface state produced exclusively lysine signals. This then provided an opportunity to investigate what structural features were responsible for the SFG result. It was determined that on each surface, the lack of signal from functional groups of the "opposite" hydrophobicity was due to their orientation in the plane of the surface, facilitated by a conformation change of the peptide backbone. We note that details of the structures predicted by the simulations are sensitive to the way the surface is represented and the choice of interaction model; a detailed comparison is presented in Ref. 24.

The availability of coordinates for all atoms in the system provide a further opportunity to investigate the role of water in mediating this interaction. Based on our previous work on the spectroscopy and simulation of neat solid–water interfaces,[27] we can determine to what extent the water structure is perturbed in the presence of the peptide. The structure of water between the hydrophilic surface and the peptide was found to vary with distance from the surface, allowing us to differentiate surface-induced, bulk-like, and peptide-induced water behaviour. Fig. 5a shows that water structure is dictated by the surface when the peptide is within 0.5 nm, as evidenced by the identical water density profiles in the absence of the peptide. However, when the peptide is 0.6 nm from the surface, the nearly constant water density and order parameter values tending towards zero indicate a bulk-like structure. Greater than 0.6 nm from the surface, the density and order profiles indicate that water structure is determined by the peptide. The orientation of water molecules close to the surface and bottom face of the peptide were found to be similar (with the oxygen atom pointing towards the peptide) as indicated by the similar positive order parameter values for

each water population (Fig. 5b). This suggests that the presence of water is favourable in mediating interactions between the hydrophilic surface and peptide. A layer of well-ordered water molecules is always present at hydrophilic surfaces whose structure is influenced by both the surface and adsorbed peptide. At hydrophobic surfaces water is excluded upon adhesion of the peptide to the surface, which are in direct contact. This is shown in Fig. 5c where there is a paucity of water when peptide atoms are 0.5 and 0.6 nm from the surface. Although the water density between the peptide and a hydrophobic surface is much lower than at a hydrophilic surface, it has a higher degree of ordering. Even when the peptide is 2 nm from the surface, the trapped water barely reaches bulk-like behaviour (Fig. 5d) which would be indicated by an order parameter of zero. However, for both hydrophobic and hydrophilic surfaces, the water was found to be oriented with its oxygen pointing toward the adhered peptide. These results shed light on the role of water in mediating biomolecular adsorption to surfaces of varying hydrophobicity.

3.2 Multi-component synthetic adhesives

We now introduce a more complex system, that of a multi-component pressure-sensitive adhesive. Such formulations are important in a wide range of household and industrial applications, especially in the construction industry where bonding between specific materials is required.[28,29] Most of these formulations include polymers.[30] One of the challenges is to balance the higher wettability and tack of low glass transition (T_g) materials, with the higher shear resistance and cohesive strength offered by high T_g materials.[31] An approach has been to add acrylic acid to low T_g poly(butyl acrylate) formulations. Water plays a critical role in such systems, as it is a major component of the formulation at the time of application, and ultimately provides the final surface interactions between adhesive molecules and the substrate as the water leaves. Techniques such as attenuated total internal reflection infrared (ATR-IR) absorption are ideal for probing water infiltration or evaporation processes as large changes in absorbance are measured when molecules enter or leave the evanescent wave probe

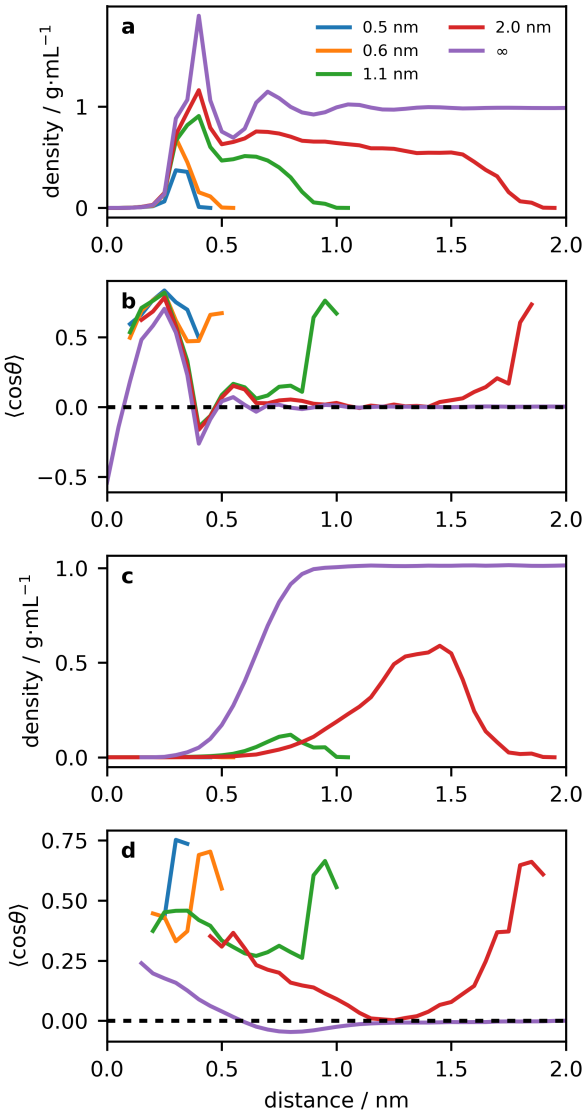

Figure 5: (a) Density and (b) polar tilt angle order parameter for water trapped between LKα14 and a hydrophilic surface. (c) Density and (d) polar tilt angle order parameter for water trapped between LKα14 and a hydrophobic surface.

volume. Such experiments are a perfect complement to SFG, as $\chi^{(2)}$ processes cannot probe sub-surface species that are not oriented. We are careful in the use of the term "bulk" here, as the composition of the material in the first few microns near the surface may be different from that further into the bulk polymer phase.

We have recently been exploring the potential of surface–bulk heterospectral correlation analysis where SFG spectra are combined with IR absorption or Raman scattering to untangle structural clues for systems where the surface ordering is triggered by changes in the bulk composition.[32,33] We calculate the complex correlation coefficient

$$C(\omega_1, \omega_2) = \Phi(\omega_1, \omega_2) + i\Psi(\omega_1, \omega_2) \tag{6}$$

where the real part,

$$\begin{aligned} \Phi(\omega_1, \omega_2) = \frac{1}{m-1} &\left[\mathbb{I}\mathrm{m}\{\chi^{(1)}(\omega_1, t_i)\} - \frac{1}{m}\sum_{i=1}^{m} \mathbb{I}\mathrm{m}\{\chi^{(1)}(\omega_1, t)\} \right] \\ &\times \left[|\chi^{(2)}(\omega_2, t_i)| - \frac{1}{m}\sum_{i=1}^{m} |\chi^{(2)}(\omega_2, t)| \right] \end{aligned} \tag{7}$$

the synchronous spectrum, is calculated from the ATR-IR $\mathbb{I}\mathrm{m}\{\chi^{(1)}\}$ and the SFG $|\chi^{(2)}|$ spectra. Eq. 7 shows that we are subtracting the mean value obtained at each wavenumber ω with respect to time t during the polymer drying process. Here ω_1 is the IR frequency in the ATR-IR experiment, and ω_2 is the IR frequency in the SFG experiment. If there are N points in the ATR-IR region of interest, and M points in each SFG spectrum, $\Phi(\omega_1, \omega_2)$ is an $N \times M$ quantity that reveals the correlation between the IR response at ω_1 with the SFG response at ω_2 for the spectra collected as a function of time. A positive cross peak in Φ indicates that the ATR-IR and SFG signal are both growing or shrinking with respect to time; a negative cross peak indicates that the signal is increasing in the bulk and decreasing at the surface, or vice versa. The imaginary part of the correlation coefficient is obtained by

a similar method

$$\Psi(\omega_1,\omega_2) = \frac{1}{m-1}\left[\mathbb{I}\mathrm{m}\{\chi^{(1)}(\omega_1,t_i)\} - \frac{1}{m}\sum_{i=1}^{m}\mathbb{I}\mathrm{m}\{\chi^{(1)}(\omega_1,t)\}\right] \times N_{ij}\cdot\left[|\chi^{(2)}(\omega_2,t_i)| - \frac{1}{m}\sum_{i=1}^{m}|\chi^{(2)}(\omega_2,t)|\right] \tag{8}$$

where N_{ij} are elements of the Hilbert-Noda transformation matrix.[34] This asynchronous component of the correlation highlights spectral changes that are phase shifted between the surface and bulk spectroscopies.[34–36]

The role of acrylic acid in determining the surface structure of a poly(butyl acrylate)-based pressure sensitive adhesive (PSA) on sapphire during the water evaporation process was studied using ATR-IR and SFG spectroscopy.[37] The synchronous and asynchronous 2D correlation maps, together with the corresponding ATR-IR and SFG spectra, are shown in Fig. 6 for the mixture without acrylic acid. We exclude the water O–H stretching region from the analysis as the water modes are very strong in the IR absorption spectra, and decrease as expected as water leaves the interfacial region. Knowing this dominant bulk water response, we analyze the C–H stretching region with the goal of interpreting the results together with the bulk water trends. Here the negative asynchronous feature together with the negative corresponding feature in the synchronous map (Fig. 6c and d) indicates that the decrease in SFG intensity occurs after the increase in IR C–H stretching mode intensities from the polymer. Thus, an accumulation of interfacial PSA precedes the ordering of the polymer, indicating that ordering at the surface is driven by packing as the water content decreases during the drying process. In contrast, when a small amount acrylic acid is added to the PSA, a positive synchronous signal, coupled with a large negative feature in the asynchronous map, signifies that the change in SFG intensity precedes any changes in IR signal. We conclude that an orientation change of the polymer occurs before an increase in surface population. As the water content decreases, the polymer rapidly reorients itself to replace previous hydrogen bonding of the acrylic acid with water, with hydrogen bonds to the O–H terminated sapphire

surface. These results provide insight into the role of water and acrylic acid in dictating the molecular level structure of PSAs adhered to surfaces, which is integral to gaining a better understanding of the performance of the materials.

3.3 Bacterial adhesives

Bacterial adhesion is a multi-faceted process governed by the nature of the surface, solution conditions, and solvation environment. A conditioning layer of proteins is first deposited, allowing cells to adhere and produce extracellular polymeric substances (EPS) which, over a period of hours to days, completely envelop the surface.[38] Secretion of EPS is one of the unique features of sessile bacteria, improving adhesion and cohesion, and offering enhanced resistance to environmental stresses.[39–41] Studies varying the surface and solution conditions have concluded that the nature of the surface, including its charge, hydrophobicity, and roughness, as well as pH and ionic strength of the environment, are critical features influencing the amount and conformation of adsorbed proteins and cells.[42,43] The solvation environment is integral for both protein and bacterial adhesion, such that changes in the hydration structure at the surface are a sensitive measure of early adhesion events. Water molecules may compete with conditioning proteins for hydrogen bonding opportunities with the surface, thereby suppressing cell adhesion.[44] Water constitutes by far the largest part of the environment in which most bacteria grow, and is also the major component of the EPS matrix. Polymers within this matrix trap ions and other osmolytes, creating microenvironments with varying nutrient and chemical gradients that are important for cell growth and eventual biofilm development.[45]

To investigate bacterial adhesion to surfaces, vibrational SFG spectroscopy, combined with bulk solution measurements and imaging, were used to study silica surface conditions during the growth of *E. Coli* K12.[17] As a result of the high surface charge density of silica near neutral pH, the water structure at the silica-aqueous interface is known to be especially sensitive to pH and ionic strength, and surface concentration profiles develop that can be

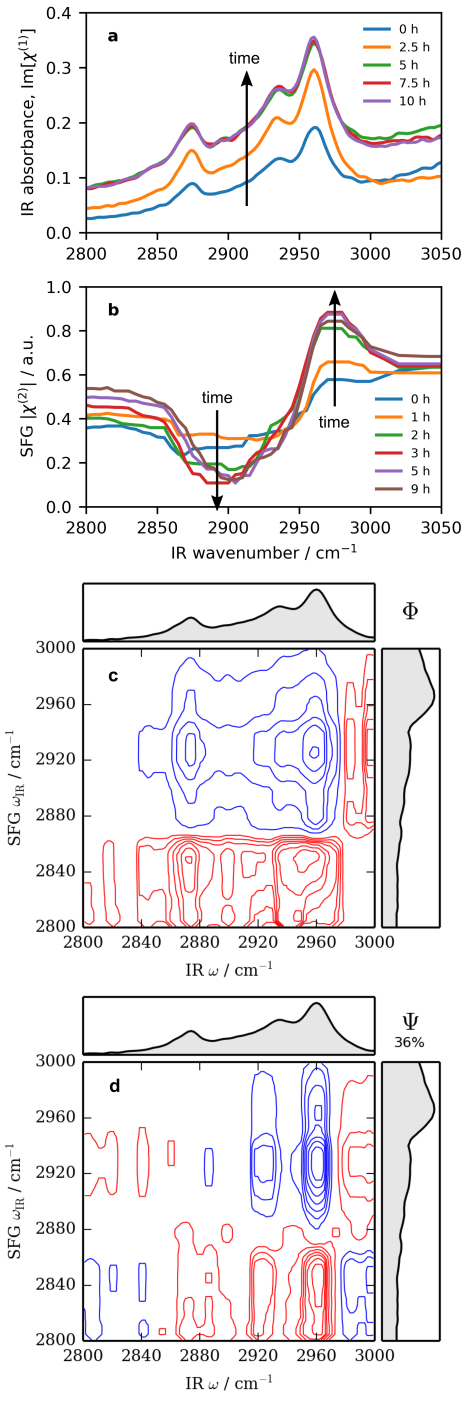

Figure 6: (a) IR absorption spectra of a pressure-sensitive adhesive collected as a function of time; (b) corresponding SFG spectra; (c) synchronous and (d) asynchronous correlation maps generated from the spectral data.

appreciably different from the bulk solution conditions. As the *E. Coli* were grown inside our SFG spectrometer and spectra collected over a 24 h period, a continual increase in the interfacial water O–H stretching was observed, as illustrated in Fig. 7a. After 24 h, the water signal reaches 53% of the silica–water signal. It was noted that the increase in SFG intensity (Fig. 7c) exactly matched the population growth curve for this bacteria (Fig. 7b).

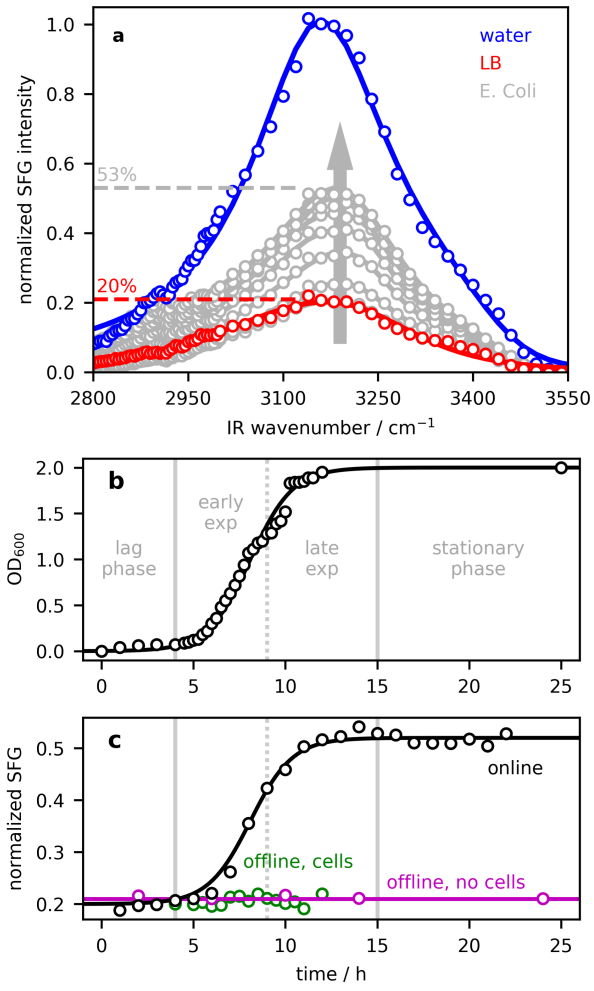

Figure 7: (a) SFG spectra collected at the aqueous-silica interface for water (blue), LB growth medium (red), and *E. Coli* K12 (grey). During the bacteria growth, SFG intensity increases from 21% of the initial silica-water signal to 53% of this level. The intensity at 3200 cm^{-1} is plotted in (c) (black points) along with analogous offline experiments with and without cells. (b)*E. Coli* K12 growth curve as determined from the optical density at 600 nm. Adapted from Ref. 17. Copyright (2018) AIP publishing.

We have proposed that, in the presence of growing cells, a unique surface microenviron-

ment is established as a result of metabolites and EPS accumulating on the silica surface (Fig. 8), attributed to a reduction in the local ionic strength as the EPS deplete ions from the region immediately adjacent to the silica. Even in the subsequent absence of the cells, this surface layer of polymers works to reduce the interfacial ionic strength as revealed by the enhanced signal from surface water molecules.[17] This occurs as a result of reduced screening of the negatively charged silica surface, producing a greater $\chi^{(3)}$ contribution to the signal. In the presence of growing cells, an additional boost in surface water signal is attributed to a local pH that is higher than that of the bulk solution. This occurs as a result of cells producing ammonium during growth,[46] which is then attracted to the negatively charged surface and becomes trapped within the microenvironment. Increases in local pH would produce a more negative silica surface charge, further enhancing the SFG signal. Bulk pH and ionic strength measurements showed small changes that were not sufficient to account for the magnitude of the observed increase in SFG intensity.[47] The formation of a microenvironment at the surface, consisting of cells, their excretion products (EPS, metabolites) and ions associated with this extracellular matrix of polymers, would result in a pH and ionic strength at the surface that is distinct from the bulk—a phenomenon common throughout the biofilm matrix. By using a surface-sensitive technique we are able to investigate changes occurring in this complex, multi-component system by monitoring the interfacial water response to adhesion.

4 Conclusion and perspectives

The role of interfacial water as both a mediator and reporter of adhesion at solid-aqueous interfaces has been demonstrated using a combination of bulk- and surface-specific vibrational spectroscopies, together with molecular simulations. For peptide adhesion at both hydrophilic and hydrophobic surfaces, simulations and spectral modeling enables interfacial structure and orientation to be determined, and informs on the influence of water in

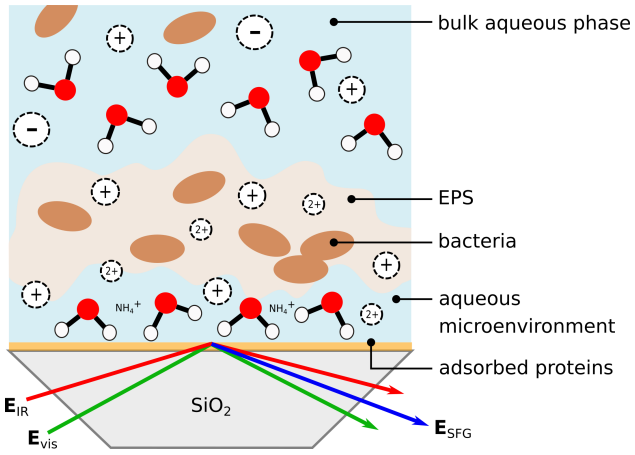

Figure 8: Illustration of the surface microenvironment created during bacterial growth and adhesion.

mediating adhesion to the surface. On hydrophilic surfaces water facilitates solvation and mediates interactions with the substrate. Combining surface- and bulk-sensitive techniques becomes important when changes in the bulk solution affect interfacial processes. We have illustrated the utility of two-dimensional correlation analysis in studying the water evaporation process of a polymer adhesive. In the case of bacterial adhesion to silica, changes in the spectral response from interfacial water were used as an indicator of changes occurring in the microenvironment separated from the bulk aqueous phase due to extracellular polymer adhesion. The use of SFG to probe the interfacial environment during bacterial adhesion is new for the biofilm community, which mostly uses vibrational techniques such as ATR-IR and Raman to study biofilm composition near the surface.

Adsorption from the aqueous phase is a complex and multi-faceted problem. For a more complete understanding, it is necessary to investigate many aspects of the system including changes occurring in the bulk water and at the interface. Coupling SFG with bulk probes such as IR, Raman, mass spectrometry, and NMR for composition analysis; AFM and ellipsometry for structural analysis, would help to better characterize heterogeneous samples. Further research combining SFG with optical and fluorescence imaging will also be important in gaining greater perspective on biological systems such as adhesion of living cells where the variability between samples presents challenges. The ability to characterize

the chemical composition of the interfacial environment, while simultaneously coupling this information to changes in the structure and morphology of adhered cells and colonies, can provide insight into cellular adhesion processes and biofilm formation.

We have also highlighted the possibility of obtaining qualitative information from SFG spectra. This represents a shift for the nonlinear vibrational spectroscopy community, where it has been established that the study of small molecules with known composition can yield remarkable quantitative detail about orientation, conformation, and the surface orientation distribution.[48,49] In contrast, by examining trends in spectral intensity changes, SFG spectra can be used to obtain information about changes occurring in the interfacial environment. Even in cases where detailed analysis of vibrational modes is not performed, optical effects such as local field corrections are critical, and must be considered. For example, when working in an internal reflection geometry near the critical angle of one or more beams, small changes in refractive index may have drastic consequences on the measured intensity. Such a local refractive index sensor may be of interest, but it is important that this contribution to the signal be recognized, and not misinterpreted as changes in the surface population or organization of molecules. Although techniques for processing data to include such effects are described in detail in the literature, there is still some discussion surrounding the nature of the correction, and experimental confirmations of the various approaches are not widely available. Nevertheless, the structure, orientation, and mechanistic information on molecular adhesion that can be gained from using these nonlinear optical techniques, and combining with other bulk probes and simulations, provides powerful tools for studying these systems. This is especially true at solid–aqueous interfaces where water is integral in mediating adhesion and its response can be used to investigate interfacial processes that occur in a wide variety of biologically, chemically, and industrially relevant systems.

Biographical Information

Tasha Jarisz obtained her B.Sc. with honours in Chemistry from the University of Victoria in 2015, and is currently a Ph.D. student in the Hore group. Her research is centered around water and biomolecular structure at silica surfaces.

Sandra Roy obtained her B.Sc. in Chemistry from Université Laval, and then joined the Hore group for her M.Sc. and Ph.D.. Her thesis investigated the correlation between surface and bulk behaviour using optical probes. Since 2018 she is a postdoctoral fellow at ETH Zurich.

Dennis Hore received his Ph.D. in Chemistry from Queen's University under the mentorship of Profs. Almeria Natansohn and Paul Rochon (Royal Military College, Physics). He was then a postdoc in Prof. Geri Richmond's group at the University of Oregon. His research interests are focused on the development of optical techniques for materials characterization.

Acknowledgement

We thank the Natural Sciences and Engineering Research Council of Canada (NSERC) for support of this science with a Discovery Grant. Equipment was purchased with assistance from the Canadian Foundation for Innovation and the British Columbia Knowledge Development Fund. Simulations were run on Compute Canada and Westgrid clusters. TAJ is grateful to NSERC for CGS-M and CGS-D scholarships.

References

1 Li, S.; Du, L.; Wei, Z.; Wang, W. Aqueous-Phase Aerosols on the Air-Water Interface: Response of Fatty Acid Langmuir Monolayers to Atmospheric Inorganic Ions. *Sci. Total Environ.* **2017**, *580*, 1155–1161.

2 Salta, M.; Wharton, J. A.; Blanche, Y.; Stokes, K. R.; Briand, J.-F. Marine Biofilms on Artificial Surfaces: Structure and Dynamics. *Environ. Microbiol.* **2013**, *15*, 2879–2893.

3 Crossley, S.; Faria, J.; Shen, M.; Resasco, D. E. Solid Nanoparticles that Catalyze Biofuel Upgrade Reactions at the Water/Oil Interface. *Science* **2010**, *327*, 68–72.

4 Pratt, L. R.; Pohorille, A. Hydrophobic Effects and Modeling of Biophysical Aqueous Solution Interfaces. *Chem. Rev.* **2002**, *102*, 2671–2692.

5 Walker, D. S.; Hore, D. K.; Richmond, G. L. Understanding the Population, Coordination, and Orientation of Water Species Contributing to the Nonlinear Optical Spectroscopy of the Vapor-Water Interface Through Molecular Dynamics Simulations. *J. Phys. Chem. B* **2006**, *110*, 20451–20459.

6 Henderson, M. A. The Interaction of Water With Solid Surfaces: Fundamental Aspects Revisited. *Surf. Sci. Rep.* **2002**, *46*, 1–308.

7 Nel, A. E.; Maedler, L.; Velegol, D.; Xia, T.; Hoek, E. M. V.; Somasundaran, P.; Klaessig, F.; Castranova, V.; Thompson, M. Understanding Biophysicochemical Interactions at the Nano-Bio Interface. *Nat. Mater.* **2009**, *8*, 543–557.

8 Soper, A. K. The Radial Distribution Functions of Water and Ice From 220 to 673 K and at Pressures Up to 400 MPa. *Chem. Phys.* **2000**, *258*, 121–137.

9 Roy, S.; Hore, D. K. Simulated Structure and Nonlinear Vibrational Spectra of Water Next to Hydrophobic and Hydrophilic Solid Surfaces. *J. Phys. Chem. C* **2012**, *116*, 22867–22877.

10 Boyd, R. W. *Nonlinear Optics*, 2nd ed.; Academic Press: San Diego, 2003.

11 Bower, D. I. Investigation of Molecular Orientation Distributions by Polarized Raman Scattering and Polarized Fluorescence. *J. Poly. Sci.* **1972**, *10*, 2135–2153.

12 Covert, P. A.; Jena, K. C.; Hore, D. K. Throwing Salt into the Mix: Altering Interfacial Water Structure by Electrolyte Addition. *J. Phys. Chem. Lett.* **2014**, *5*, 143–148.

13 Raymond, E. A.; Tarbuck, T. L.; Richmond, G. L. Isotopic Dilution Studies of the Vapor/Water Interface as Investigated by Vibrational Sum-Frequency Spectroscopy. *J. Phys. Chem. B* **2002**, *106*, 2817–2820.

14 Scatena, L. F.; Brown, M. G.; Richmond, G. L. Water at Hydrophobic Surfaces: Weak Hydrogen Bonding and Strong Orientation Effects. *Science* **2001**, *292*, 908–912.

15 Segelstein, D. J. The Complex Refractive Index of Water. M.Sc. thesis, University of Missouri, Kansas City, 1981.

16 Warren, S. G. Optical Constants of Ice From the Ultraviolet to the Microwave. *Appl. Opt.* **1984**, *23*, 1206–1225.

17 Jarisz, T. A.; Lane, S.; Gozdzialski, L.; Hore, D. K. Ions, Metabolites, and Cells: Water as a Reporter of Surface Conditions During Bacterial Growth. *J. Chem. Phys.* **2018**, *148*, 222825.

18 Ehrenstein, G.; Lecar, H. Electrically Gated Ionic Channels in Lipid Bilayers. *Q. Rev. Biophys.* **1977**, *10*, 1–34.

19 DeGrado, W. F.; Lear, J. D. Induction of Peptide Conformation at Apolar Water Interfaces. 1. A Study with Model Peptides of Defined Hydrophobic Periodicity. *J. Am. Chem. Soc.* **1985**, *107*, 7684–7689.

20 Phillips, D. C.; York, R. L.; Mermut, O.; McCrea, K. R.; Ward, R. S.; Somorjai, G. A. Side Chain, Chain Length, and Sequence Effects on Amphiphilic Peptide Adsorption at Hydrophobic and Hydrophilic Surfaces Studied by Sum-Frequency Generation Vibrational Spectroscopy and Quartz Crystal Microbalance. *J. Phys. Chem. C* **2007**, *111*, 255–261.

21 Mermut, O.; Phillips, D. C.; York, R. L.; McCrea, K. R.; Ward, R. S.; Somorjai, G. A. In Situ Adsorption Studies of a 14-Amino Acid Leucine-Lysine Peptide onto Hydrophobic Polystyrene and Hydrophilic Silica Surfaces Using Quartz Crystal Microbalance, Atomic Force Microscopy, and Sum Frequency Generation Vibrational Spectroscopy. *J. Am. Chem. Soc.* **2006**, *128*, 3598–3607.

22 Weidner, T.; Breen, N. F.; Li, K.; Drobny, G. P.; Castner, D. G. Sum Frequency Generation and Solid-State NMR Study of the Structure, Orientation, and Dynamics of Polystyrene-Adsorbed Peptide. *Proc. Natl. Acad. Sci. U.S.A.* **2010**, *107*, 13288–13293.

23 Weidner, T.; Castner, D. G. SFG Analysis of Surface Bound Proteins: A Route Towards Structure Determination. *Phys. Chem. Chem. Phys.* **2013**, *15*, 12516–12524.

24 Collier, G.; Vellore, N. A.; Yancey, J. A.; Stuart, S. J.; Latour, R. A. Comparison Between Empirical Protein Force Fields for the Simulation of the Adsorption Behavior of Structured LK Peptides on Functionalized Surfaces. *Biointerphases* **2012**, *7*, 1–19.

25 Deighan, M.; Pfaendtner, J. Exhaustively Sampling Peptide Adsorption with Metadynamics. *Langmuir* **2013**, *29*, 7999–8009.

26 Roy, S.; Naka, T. L.; Hore, D. K. Enhanced Understanding of Amphipathic Peptide Adsorbed Structure by Modeling of the Nonlinear Vibrational Response. *J. Phys. Chem. C* **2013**, *117*, 24955–24966.

27 Krause, K. D.; Roy, S.; Hore, D. K. Interplay Between Adsorbed Peptide Structure, Trapped Water, and Surface Hydrophobicity. *Biointerphases* **2017**, *12*, 02D407.

28 Sharif, A.; Mohammadi, N.; Nekoomanesh, M.; Jahani, Y. The Role of Interfacial Interactions and Loss Function of Model Adhesives on Their Adhesion to Glass. *J. Adhes. Sci. Technol.* **2002**, *16*, 33–45.

29 Awaja, F.; Gilbert, M.; Kelly, G.; Fox, B.; Pigram, P. J. Adhesion of Polymers. *Prog. Polym. Sci.* **2009**, *34*, 948–968.

30 Tobing, S. D.; Klein, A. Molecular Parameters and Their Relation to the Adhesive Performance of Acrylic Pressure-Sensitive Adhesives. *J. Appl. Polym. Sci.* **2000**, *79*, 2230–2244.

31 Ghim, D.; Kim, J. H. Effects of Composition and Layer Thickness of a Butyl Acrylate/Acrylic Acid Copolymer on the Adhesion Properties. *Korean J. Chem. Eng.* **2016**, *33*, 707–710.

32 Roy, S.; Covert, P. A.; Jarisz, T. A.; Chan, C.; Hore, D. K. Surface–Bulk Vibrational Correlation Spectroscopy. *Anal. Chem.* **2016**, *88*, 4682–4691.

33 Roy, S.; Beutier, C.; Hore, D. Combined IR-Raman vs Sum-Frequency Heterospectral Correlation Spectroscopy. *J. Mol. Struct.* **2018**, *1161*, 403–411.

34 Noda, I.; Ozaki, Y. *Two-Dimensional Correlation Spectroscopy: Applications in Vibrational and Optical Spectroscopy*; John Wiley & Sons, Ltd: San Francisco, 2004.

35 Noda, I. Two-Dimensional Infrared Spectroscopy. *J. Am. Chem. Soc.* **1989**, *111*, 8116–8118.

36 Noda, I. Two-Dimensional Infrared (2D IR) Spectroscopy of Synthetic and Biopolymers. *Bull. Am. Phys. Soc.* **1986**, *31*, 520–524.

37 Roy, S.; Freiberg, S.; Leblanc, C.; Hore, D. K. Surface Structure of Acrylate Polymer Adhesives. *Langmuir* **2017**, *33*, 1763–1768.

38 Sutherland, I. W. Biofilm Exopolysaccharides: A Strong and Sticky Framework. *Microbiol.* **2001**, *147*, 3–9.

39 Ceri, H.; Olson, M. E.; Stremick, C.; Read, R. R.; Morck, D.; Buret, A. The Calgary Biofilm Device: New Technology for Rapid Determination of Antibiotic Susceptibilities of Bacterial Biofilms. *J. Clin. Microbiol.* **1999**, *37*, 1771–1776.

40 Simoes, M. Antimicrobial Strategies Effective Against Infectious Bacterial Biofilms. *Curr. Med. Chem.* **2011**, *18*, 2129–2145.

41 Shen, Y. Antimicrobial Efficacy of Chlorhexidine Against Bacteria in Biofilms at Different Stages of Development. *J. Endodontics* **2011**, *37*, 657–661.

42 Renner, L. D.; Weibel, D. B. Physicochemical Regulation of Biofilm Formation. *MRS Bull.* **2011**, *36*, 347–355.

43 Yee, N.; Fein, J. B.; Daughney, C. J. Experimental Study of the pH, Ionic Strength, and Reversibility Behaviour of Bacteria-Mineral Adsorption. *Geochim. Cosmochim. Acta* **2000**, *64*, 609–617.

44 Norde, W.; Lyklema, J. Protein Adsorption and Bacterial Adhesion to Solid Surfaces: A Colloid-Chemical Approach. *Colloids Surf.* **1989**, *38*, 1–13.

45 Eboigbodin, K. E.; Biggs, C. A. Characterization of the Extracellular Polymeric Substances Produced by *Escherichia Coli* Using Infrared Spectroscopic, Proteomic, and Aggregation Studies. *Biomacromolecules* **2008**, *9*, 686–695.

46 Sezonov, G.; Joseleau-Petit, D.; D'Ari, R. Escherichia Coli Physiology in Luria-Bertani Broth. *J. Bacteriol.* **2007**, *189*, 8746–8749.

47 Darlington, A. M.; Jarisz, T. A.; DeWalt-Kerian, E. L.; Roy, S.; Kim, S.; Azam, M. S.; Hore, D. K.; Gibbs, J. M. Separating the pH-Dependent Behavior of Water in the Stern and Diffuse Layers with Varying Salt Concentration. *J. Phys. Chem. C* **2017**, *121*, 20229–20241.

48 Hall, S. A.; Jena, K. C.; Covert, P. A.; Roy, S.; Trudeau, T. G.; Hore, D. K. Molecular-Level Surface Structure from Nonlinear Vibrational Spectroscopy Combined with Simulations. *J. Phys. Chem. B* **2014**, *118*, 5617–5636.

49 Hofmann, M. J.; Koelsch, P. In *Soft Matter at Aqueous Interfaces*; Lang, P., Liu, Y., Eds.; Springer: New York, 2016; Chapter 15, pp 491–514.

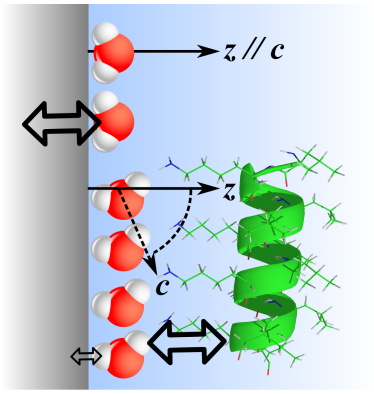
z // c
z
c